

# Ultrafast spectroscopic imaging of exfoliated graphene

Giulia Grancini<sup>1</sup>, Nicola Martino<sup>1</sup>, Massimiliano Bianchi<sup>2</sup>, Laura Giorgia Rizzi<sup>2</sup>, Valeria Russo<sup>3</sup>, Andrea Li Bassi<sup>1,3</sup>, Carlo Spartaco Casari<sup>1,3</sup>, Annamaria Petrozza<sup>1</sup>, Roman Sordan<sup>2</sup>, and Guglielmo Lanzani<sup>\*1</sup>

<sup>1</sup>Center for Nano Science and Technology@PoliMi, Istituto Italiano di Tecnologia, Via Giovanni Pascoli, 70/3, 20133 Milano, Italy

<sup>2</sup>L-NESS, Department of Physics, Polo di Como, Politecnico di Milano, Via Anzani 42, 22100 Como, Italy

<sup>3</sup>Department of Energetics, Politecnico di Milano, Via Lambruschini 4, 20156 Milano, Italy

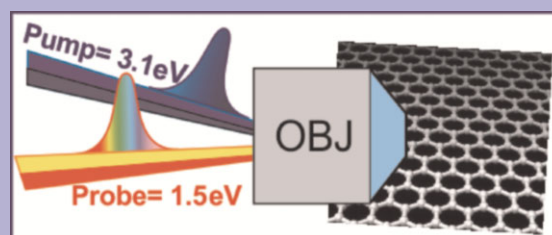
Received 30 April 2012, revised 3 August 2012, accepted 14 September 2012

Published online 1 November 2012

**Keywords** carriers cooling, graphene, transient absorption imaging, ultrafast dynamics

\* Corresponding author: e-mail [guglielmo.lanzani@iit.it](mailto:guglielmo.lanzani@iit.it), Phone: +39 02 2399 9872, Fax: +39 02 2399 6126

In this paper we investigate the carrier cooling dynamics in graphene flakes exploiting ultrafast transient absorption imaging technique. This tool enables us to combine nanoscale spatial resolution and sub-picosecond (ps) time resolution. It provides many advantages over the standard transient absorption techniques because it directly investigates the excited state dynamics at a local scale that would be usually averaged out. The local dynamics show a photobleaching recovery in the first ps, assigned to cooling by electron–phonon scattering. We found that the photoexcited carrier dynamics is spatially uniform over the micrometer-sized exfoliated graphene layer.



Ultrafast pump–probe technique is combined with an optical microscope to investigate the local excited state dynamics in graphene flakes.

© 2012 WILEY-VCH Verlag GmbH & Co. KGaA, Weinheim

**1 Introduction** Graphene is a single flat layer of carbon atoms [1], arranged in the honeycomb lattice with exciting optoelectronic properties [2–4] that make it an appealing material for nano-electronics [5, 6]. Small flakes obtained by micromechanical cleavage are difficult to be located on large substrates, and in principal should exhibit edge effects, as detected by Raman spectroscopy, due to discontinuity, defects, and variable geometry (zig-zag vs. armchair edges) [7, 8]. The edge effects triggered our interest in locally imaging the excited electron cooling dynamics on the micromechanically cleaved graphene flakes. For this reason we applied our recently developed *femtoscope* [9–11] technique to a graphene sample deposited on aluminum substrate. Our *femtoscope* is based on a combination of broadband femtosecond pump–probe spectroscopy and confocal microscopy, delivering simultaneously high temporal ( $\approx 150$  fs) and spatial resolution ( $\approx 300$  nm) [12]. In the following the basic characteristics of the experimental setup are discussed and the dynamical-imaging abilities are

shown. Our measurements demonstrate that carrier cooling is uniform across the graphene flake, and provide a clear description of the carrier dynamics in micromechanically cleaved graphene flakes.

**2 Experimental method: Ultrafast imaging** The experimental setup of the *femtoscope* is shown in Fig. 1. It is driven by 10  $\mu$ J, 150 fs pulses at 1 kHz repetition rate and 800 nm wavelength produced by an amplified Ti:Sapphire laser (Quantronix model Integra-C). The fraction of the pulse energy reflected by a first beam splitter (BS1 in the figure) is focused on a second-harmonic crystal to generate the pump pulses at 400 nm. The transmitted part is focused in a sapphire plate to produce a single-filament white light continuum spanning the 450–800 nm wavelength range, used as a probe pulse. Pump and probe beams, synchronized by a computer-controlled delay line with  $\approx 5$  fs accuracy, are collinearly recombined by a dichroic beam splitter (BS2 in the figure) and focused on the sample by a high numerical

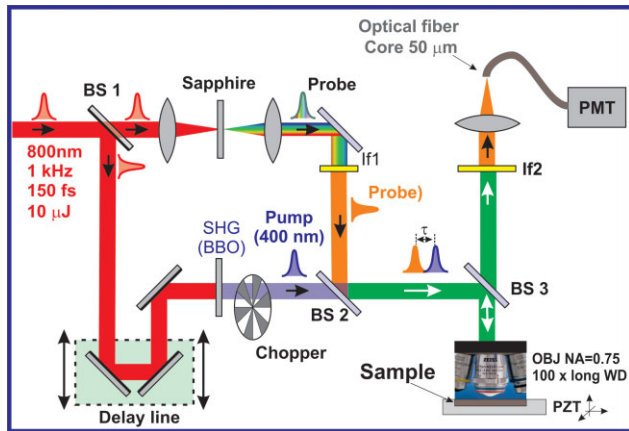


**Figure 1** (online color at: [www.pss-b.com](http://www.pss-b.com)) Experimental set-up of the ultrafast confocal microscope. BS1, BS2, and BS3, beam splitters; SHG, second harmonic generation crystal; IF1 and IF2, interference filters; OBJ, microscope objective; PZT, piezo-translator; PMT, photomultiplier.

aperture air microscope objective ( $NA = 0.75$ , magnification  $100\times$ ). The sample films are prepared on a reflective metal substrate, so that the reflection becomes equivalent to a double-pass transmission. The probe light, collected by the same microscope objective in a standard *epi* configuration, is then transmitted by BS3, spectrally filtered to reject the pump light, focused on the  $50\ \mu\text{m}$  core of an optical fiber, serving as the pinhole of the confocal microscope, and detected by a photomultiplier. Due to the chromatic aberrations of the focusing objective, pump, and probe beams have different focal planes. The sample is raster scanned by a piezo-translator with nm accuracy on a  $100\ \mu\text{m} \times 100\ \mu\text{m}$  scan area, thus allowing the acquisition of three-dimensional linear reflection  $R(x, y, \lambda)$  images as a function of sample position  $(x, y)$  and probe wavelength  $\lambda$ . By modulating the pump beam with a mechanical chopper and demodulating the collected probe light at the same frequency, we also simultaneously register four-dimensional differential reflection  $\Delta R/R(x, y, \lambda, \tau)$  images, which also depend on the pump-probe delay  $\tau$ . The minimum detectable signal is  $\Delta R/R \approx 10^{-4}$ . Our instrumental temporal and spatial resolutions are 150 fs and 300–400 nm, depending on probe wavelength, respectively.

**3 Results and discussion** Figure 2a shows the optical reflection map of a selected exfoliated graphene layer, while Fig. 2b shows the  $\Delta R/R$  signal at 200 fs pump-probe delay and at 800 nm probe wavelength on the same region, collected with our *femtoscope*. In Fig. 2a the highlighted region corresponds to a graphene monolayer, previously identified by Raman spectroscopy [13]. Figure 2b shows a positive signal (reddish in the map) corresponding to the graphene flakes. Thus, we selected three different points as indicated in Fig. 2b. This signal can be related to photobleaching from Pauli-blocking effect occurring upon

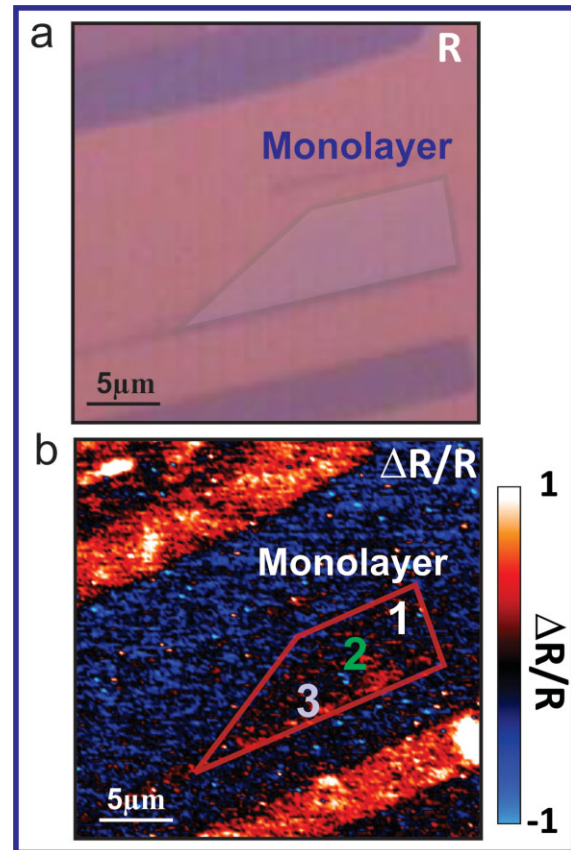


**Figure 2** (online color at: [www.pss-b.com](http://www.pss-b.com)) (a) Standard reflection optical image on  $25 \times 25\ \mu\text{m}^2$  area; (b)  $\Delta R/R(x, y)$  map at  $\tau = 200$  fs pump-probe delay collected in the same  $25 \times 25\ \mu\text{m}^2$  area of the graphene monolayer at  $\lambda = 800$  nm probe wavelength; scale-bar  $5\ \mu\text{m}$ . The solid lines represent an eye-guide contour to easily recognize the graphene layers.

photon-excitation [14, 15]. As schematically depicted in Fig. 3a, our pump pulse excites an electronic population in the conduction band. The excited electrons thermalize by scattering with optical phonons within few tens of femtoseconds reaching a quasi-equilibrium distribution at high electronic temperature (above 1000 K) [16–18]. The hot distribution subsequently cools down interacting with the acoustic phonons and possibly with the substrate. This cooling usually occurs within the first picoseconds (ps) [19–21]. The first mechanism is too rapid to be followed by our temporal resolution, while the cooling process can be monitored by looking at the pump-probe dynamics. Moreover, thanks to the sub-micron spatial resolution our *femtoscope* enables us to locally probe these dynamics at different points of the graphene layer.

In Fig. 3b the dynamics relative to the different points selected in the monolayer region are shown. In the inset the weak signal on the bare substrate is also shown. We find that the normalized dynamics at the selected points (1, 2, 3 in Fig. 2b) show a similar decay. In particular, moving from the edge region (1 and 3) towards the central part (2) of the flake

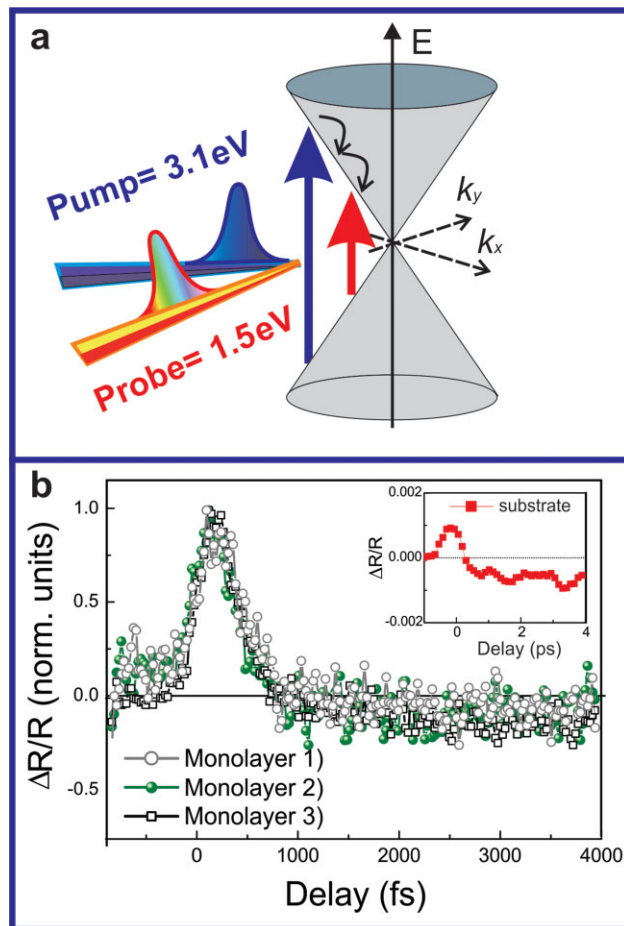


**Figure 3** (online color at: [www.pss-b.com](http://www.pss-b.com)) Photoexcited carrier dynamics in graphene. (a) Scheme of the pump probe tool to investigate the photophysics of graphene, across the Dirac point. (b)  $\Delta R/R(\lambda, \tau)$  normalized dynamics at the selected points (1)–(3) on the monolayer, as indicated in Fig. 2b. Inset: the dynamics taken on the bare substrate is shown.

they exhibit a similar fast component completed in the first picosecond. The only slight difference (evident from the map in Fig. 2b) appears in the magnitude of the signal from point 3. This is due to the presence of a fold in the bottom part of the layer, which causes no changes in the dynamics, but only an increase in the pump–probe signal intensity. The uniform behavior excludes the presence of local geometry and edge effects that can be possibly averaged out by our confocal spot. However, the dynamics clearly reveal that in this case the exfoliated graphene cooling dynamics are independent of the local morphology and occur with a time constant of about 400 fs.

In conclusion, ultrafast dynamics on exfoliated graphene are here presented monitoring the electron–phonon coupling in the first ps timescale after photon-excitation and reveal a

spatially uniform behavior on the scanned graphene layer. We envisage that our *femtoscope* can enable a further local investigation on graphene flakes where the local morphological properties are tuned to address specific electronic properties of the material.

## References

- [1] K. Novoselov, A. Geim, S. Morozov, D. Jiang, Y. Zhang, S. Dubonos, I. Grigorieva, and A. Firsov, *Science* **306**, 666–669 (2004).
- [2] A. K. Geim and K. S. Novoselov, *Nature Mater.* **6**, 183–191 (2007).
- [3] F. Miao, S. Wijeratne, Y. Zhang, U. C. Coskun, W. Bao, and C. N. Lau, *Science* **317**, 1530–1533 (2007).
- [4] F. Bonaccorso, Z. Sun, T. Hasan, and A. C. Ferrari, *Nature Photon.* **4**, 611–622 (2010).
- [5] R. Sordan, F. Traversi, and V. Russo, *Appl. Phys. Lett.* **94**, 073305 (2009).
- [6] F. Traversi, V. Russo, and R. Sordan, *Appl. Phys. Lett.* **94**, 223312 (2009).
- [7] Y. You, Z. Ni, T. Yu, and Z. Shen, *Appl. Phys. Lett.* **93**, 163112 (2008).
- [8] C. Casiraghi, A. Hartschuh, H. Qian, S. Piscanec, C. Georgi, A. Fasoli, K. S. Novoselov, D. M. Basko, and A. C. Ferrari, *Nano Lett.* **9**, 1433–1441 (2009).
- [9] D. Polli, G. Grancini, J. Clark, M. Celebrano, T. Virgili, G. Cerullo, and G. Lanzani, *Adv. Mater.* **22**, 3048–3051 (2010).
- [10] G. Grancini, D. Polli, D. Fazzi, J. Cabanillas-Gonzalez, G. Cerullo, and G. Lanzani, *J. Phys. Chem. Lett.* **2**, 1099–1105 (2011).
- [11] L. Huang, G. V. Hartland, and L.-Q. Chu, Luxmi, R. M. Feenstra, C. Lian, K. Tahy, H. Xing, and *Nano Lett.* **10**, 1308–1313 (2010).
- [12] J. Cabanillas-Gonzalez, G. Grancini, and G. Lanzani, *Adv. Mater.* **23**, 5468–5485 (2011).
- [13] A. C. Ferrari, *Solid State Commun.* **143**, 47–57 (2007).
- [14] J. M. Dawlaty, S. Shivaraman, M. Chandrashekhara, F. Rana, and M. G. Spencer, *Appl. Phys. Lett.* **92**, 042116 (2008).
- [15] R. W. Newson, J. Dean, B. Schmidt, and H. M. van Driel, *Opt. Express* **17**, 2326–2333 (2009).
- [16] M. Breusing, C. Ropers, and T. Elsaesser, *Phys. Rev. Lett.* **102**, 086809 (2009).
- [17] M. Breusing, S. Kuehn, T. Winzer, E. Malić, F. Milde, N. Severin, J. P. Rabe, C. Ropers, A. Knorr, and T. Elsaesser, *Phys. Rev. B* **83**, 153410 (2011).
- [18] S. Butscher, F. Milde, M. Hirtshulz, E. Malić, and A. Knorr, *Appl. Phys. Lett.* **91**, 203103 (2007).
- [19] H. Wang, J. H. Strait, P. A. George, S. Shivaraman, V. B. Shields, M. Chandrashekhara, J. Hwang, F. Rana, M. G. Spencer, C. S. Ruiz-Vargas, and J. Park, *Appl. Phys. Lett.* **96**, 081917 (2010).
- [20] P. A. George, J. Strait, J. Dawlaty, S. Shivaraman, M. Chandrashekhara, F. Rana, and M. G. Spencer, *Nano Lett.* **8**, 4248–4251 (2008).
- [21] L. Huang, B. Gao, G. Hartland, M. Kelly, and H. Xing, *Surf. Sci.* **605**, 1657–1661 (2011).